Notch Effects in Low Cycle Fatigue of Steels

Kunihiro IDA*, *Member*

Abstract

Results of researches made for the purpose of investigating notch effects in low cycle fatigue of steels are summarized in this paper. In the first half part, low cycle fatigue behaviour of notched wide plates subjected to repeated tensile load are described, and the crack initiation life of a notched wide plate is discussed in the correlation with the crack initiation life of a hourglass shaped, small size specimen, which was strain cycled by duplicating strain histories at the tip of notch in the wide plate.

The latter half part deals with the results of completely reversed, strain and load cycling tests of mild and 80 kg/mm² steels. One of the conclusions obtained is that the fatigue strength reduction factor defined in strain cycling of smooth and grooved specimens is approximately equal to the plastic strain concentration factor of the notch.

List of Symbols

K_t : Elastic stress concentration factor of a notch

K_σ : Plastic stress concentration factor of a notch

K_ϵ : Plastic strain concentration factor of a notch

K_f : Fatigue strength reduction factor

n : Number of stress (or strain) cycles imposed

N_c : Visible crack initiation life; number of cycles to initiate a surface crack 0.2 to 0.5 mm in length

$N_c(H)$: Visible crack initiation life of hourglass specimen fatigued by strain cycles with reproduced strain history at the notch root in wide plate

$N_c(P)$: Visible crack initiation life of notched wide plate

N_e : Expected visible crack initiation life of notched wide plate on the basis of results of small size specimens of solid cylinder

N_f : Failure life; number of cycles to complete failure of a specimen

ΔN : Number of cycles in a step

S_a : Amplitude of net section stress in load-controlled fatigue (kg/mm²)

S_R : Range of net section stress in load-controlled fatigue (kg/mm²)

a, m and p: Material constants

ϵ_f : Static fracture ductility ($=\ln\{100/(100-RA)\}$, RA=reduction in area in percent)

ϵ_m : Mean strain in strain cycling test

ϵ_{m0} : Mean strain at the end of 1st or 2nd cycle

ϵ_{ea} : Longitudinal, natural elastic strain amplitude

ϵ_{pa} : Longitudinal, natural plastic strain amplitude

ϵ_{ta} : Longitudinal, natural total strain amplitude

ϵ_{tR} : Longitudinal, natural total strain range

ϵ_{ta}^d : Diametral, natural total strain amplitude

ϵ_{ta}^r : Radial, natural total strain amplitude

$\epsilon_{eq,a}$: Equivalent, natural, total strain amplitude

$\Delta\epsilon_m$: Increment of mean strain

σ_y : Yield stress (kg/mm²)

σ_u : Nominal ultimate tensile strength (kg/mm²)

σ_f : Static true fracture strength (kg/mm²)

* Professor, Department of Naval Architecture, Faculty of Engineering, University of Tokyo

1. Introduction

The estimation methods of low cycle fatigue strength of a structure may be classified into two groups. The first one is a method of gaining direct information about the fatigue strength of a structure by carrying out load-controlled low cycle fatigue tests, or displacement-controlled low cycle fatigue tests in particular cases, of scale models of structural components and notched wide plates. The second method, that may be regarded as a so-called indirect method, is to predict the fatigue strength of a structure by using basic fatigue diagrams, which are obtained by strain-controlled low cycle fatigue tests of cylindrical specimens of small size. The basis of the second method may be provided by the experimental fact that local strain at a notch behaves, in general, in roughly constant range of strain.

In the former case, the strength comparison between specimen series will be very apt to be based on the qualitative judgement, because it is generally difficult to conduct fatigue tests of many specimens in any test series due to restrictions of testing period and expenses. Although the second method is adopted in a structural design code such as Section III of the ASME Boiler and Pressure Vessel Code, weak points of the method are mentioned as follows: (1) It is rather difficult to prove scale effects involving influences of yield zone size that depends upon material properties, (2) Uneasiness is felt about to what extent could controlling conditions in strain cycling of a small size specimen duplicate strain cycle history at a notch in a realistic structure, and (3) To what extent should the value of safety factor be evaluated in the application of basic fatigue diagrams for design purpose.

If the problem is simplified for the simplest case where a notched wide plate is subjected to tensile load, one question should be raised on what kind of strain history must be applied to a small size specimen tested in strain cycling in order to obtain the same fatigue life for both a notched wide plate and a cylindrical specimen of small size. Very few researches, however, have been made from such viewpoint. Crews et al.[1] cycled side notched, $K_t=2$, 2024-T3 aluminum-alloy sheet specimens until local stress conditions stabilized, and reproduced the plastic strain histories in simple, unnotched specimens of small size. The results by Crews et al. show good agreement between actual failure life of notched sheet specimen and life predicted by the results of unnotched, solid and cylindrical specimens in lower life range up to approximately 3×10^4 cycles, while the agreement is poor in higher life range.

The necessity of researches from such point of view should be easily recognized for ship structure steels, and this recognition afforded the starting point of the investigation of which results are described in the first half part of the present paper.

The next problem concerns the fatigue strength reduction factor caused by a sharp notch, which is located in a structural discontinuity of small value of elastic stress concentration factor. In other words, the problem relates to notch effects in strain cycling. The local and superposed influences of gas cut notch, undercuts and weld defects, which are located in the region of structural notch, on the low cycle fatigue strength may be cited as examples.

The accurate information about fatigue strength reduction factor in low cycle fatigue must be one of the important factors in fatigue design of a structure. If the allowable stress could be increased by precise design with smaller safety factor, overestimation of the fatigue strength reduction factor leads to loss of design stress. On the contrary, underestimation of the factor will cause unsafe design. Relating to this problem, the Nuclear Power Piping Code of USA Standard, USAS-B31.7 (1969), defined the A-factor for use in simplified elastic-plastic analysis. The A-factor, that is the ratio of (K_f-K_t) to (K_t-1), is expressed in graphs as a function of primary plus secondary stress intensity for carbon steel, 2−1/4 Cr−1 Mo

steel and 304 stainless steel. It seems construction of A-factor curves were based on a Targart's paper[2] in which analysis was made about the results obtained by Krempl[3]. One subject to be discussed here is if A-factor curves given in USAS-B31.7 Code could be applicable to other steels than those mentioned in the Code. Incidentally, A-factor was changed to K_e-factor, in Section III of ASME Boiler and Pressure Vessel Code (1971), with some modification of definition.

A paper published in 1965 by Manson and Hirschberg[4] may be the first instance of researches on the fatigue strength reduction factor in low cycle fatigue. After that several papers have been published, and the results of them are divided into two groups: the one concludes the fatigue strength reduction factor is equal to or lower than the elastic stress concentration factor, while the other leads the conclusion that the former is always higher than the latter.

For the purpose of obtaining a basis for definite interpretation of the fatigue strength reduction factor in low cycle fatigue, investigations of which results are summarized in the latter half part of the present paper was made by carrying out strain- and load-controlled low cycle fatigue tests of smooth and notched specimens of the same steels.

Thus the present paper deals mainly with condensed results of researches[5),6),7),8)] which had been carried out by the author and his co-workers in order to investigate the notch effects in low cycle fatigue of ship structure steels.

Table 1 Chemical Compositions of Steels (Ladle Analysis; Percent by Weight)

Steel	C	Mn	Si	P	S
SM41B	0.20	0.71	0.06	0.11	0.23
SM50B	0.17	1.34	0.32	0.20	0.11

2. Prediction of Fatigue Life of Notched Plate[6),7)]

2.1 *Experimental Details*

Two commercial steels of 13 mm in thickness were tested in the as-received condition: a mild steel, SM41B steel specified in the JIS Code, and a 50 kg/mm² high strength steel, SM50B steel specified in the JIS Code. Chemical compositions and mechanical properties of the two materials are listed in Tables 1 and 2, respectively.

Figure 1 shows dimensions of notched wide plate specimens. A notch was machined at the center of a specimen. The configurations of three notches, type A, B and C, give elastic stress concentration factor of approximately 5, 10 and 14, respectively with the assumption of an ellipse or a slot with round corners in an infinite plate[9].

From the same materials hourglass type

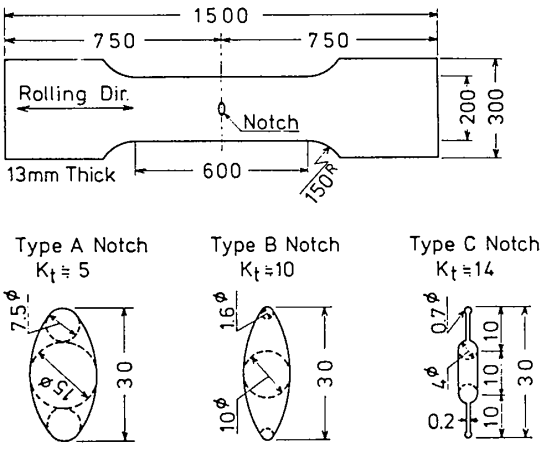

Fig. 1 Details of Notched Wide Plate Specimens

Table 2 Tensile Properties of Steels (Mean Value of Static Tension Test Results of Hourglass Type Specimens)

Steel	Material Code	σ_y (kg/mm²)	σ_u (kg/mm²)	σ_f (kg/mm²)	ϵ_f
SM41B	M	27.5	44.6	97.0	0.887
SM50B	H	36.1	53.4	114.8	1.184

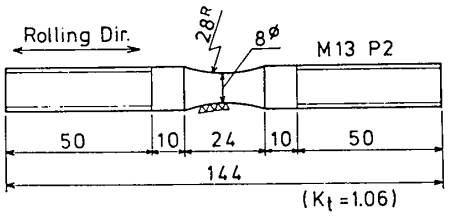

Fig. 2 Details of Hourglass Shaped Specimen

specimens, of which configuration is shown in Fig. 2, were also machined out for the use in strain-controlled low cycle fatigue tests.

Each one of all the notched plate specimen series was tested by static tensile load, and strain distributions on front and rear surfaces of the notched section were measured at maximum and minimum loads by using strain gauges and Moiré method. With reference to the method used by Nagai et al.[10], gratings of 150 lines/inch were photoengraved on specimen surface, and change of grating was photographed during the test. By extending the technique developed by Bossaert et al.[11] to linear mismatching method, strain analysis was made for interference fringe lines which were made on an enlarged photograph by mismatching.

Controlled repeated axial load was applied to the notched wide plate specimen until a fatigue crack up to 0.5 mm in length will initiate at a notch corner, and after that the specimen was loaded under the condition of constant maximum load or of constant maximum net section stress.

Hourglass shaped specimens with the configuration of 8 mm in diameter and 1.06 in shape factor[12] were tested in strain cycling. In the test, a cyclic strain history, that was previously obtained at the tip of a notch in a plate specimen subjected to repeated axial loading, was duplicated in a hourglass type specimen.

2.2 *Results and Discussion*

2.2.1 *Cyclic Characteristics of Peak Strains*

Figures 3, 4, and 5 show cyclic characteristics of longitudinal peak strain measured by Moiré method at the tip of a notch in wide plate specimen. In these figures the specimen code is given as follows: *M* for mild steel, *H* for 50 kg/mm² high tensile steel, *A*, *B* and *C* for notch configurations as shown in Fig. 1.

In case of the mild steel specimens, maxi-

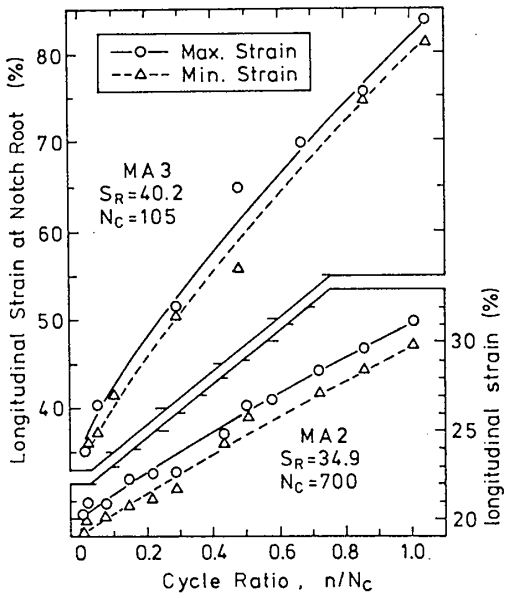

Fig. 3 Cyclic Characteristics of Longitudinal Strain at the Tip of Notch (Mild Steel Specimens; $K_t=5$)

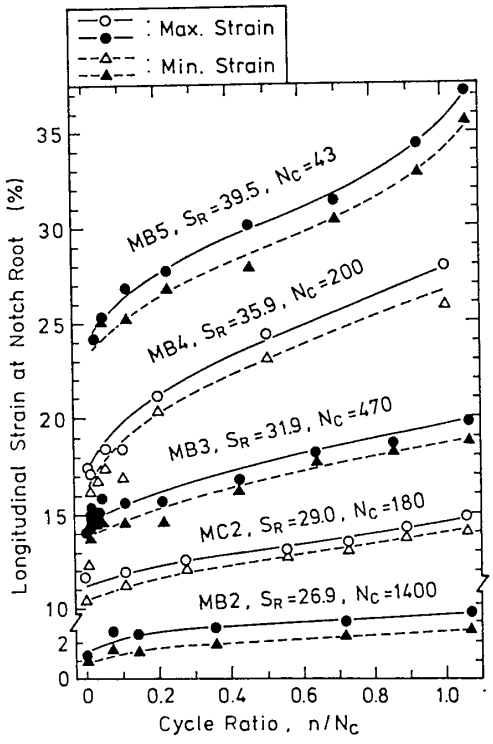

Fig. 4 Cyclic Characteristics of Longitudinal Strain at the Tip of Notch (Mild Steel Specimens; $K_t=10$ and 14)

mum and minimum strains increased greately in the range of imposed cycles less than one tenth of the crack initiation life, and after that showed nearly constant increasing rate. On the contrary, nearly linear increasing tendency is observed in the whole range of cycle ratio for the 50 kg/mm² strength steel. Another tendency, which is observed for both steels, is that the strain range at the tip of a notch is found to be approximately constant until the crack initiation.

Closer observation about crack initiation behaviour proved that the crack initiation life of a notched wide plate could be affected by four factors: (1) The maximum peak strain at the first half cycle, (2) Amplitude of peak strain, (3) Increasing mean strain at the tip of a notch and (4) The degree of restraint in thickness direction. For example, in case of a specimen with K_t of 10, a fatigue crack initiated at an early stage at the thickness center of a notch root, and the crack extended in thickness direction from both ends of it. During this period no crack was observed on specimen surfaces. In case of a specimen with K_t of 5, five to ten cracks of about 1 mm long were developed at an early stage on the surface of a notch root, and some of these cracks extended their length, while the rest cracks stayed with their original lengths. During this period a crack of approximately 0.5 mm long initiated independently on a specimen surface at a tip corner of the notch. Thus, the crack initiation life of a notched wide plate specimen $N_c(P)$ was defined as the number of cycles to initiate a crack up to 0.5 mm long at a corner of tip of a pre-machined notch.

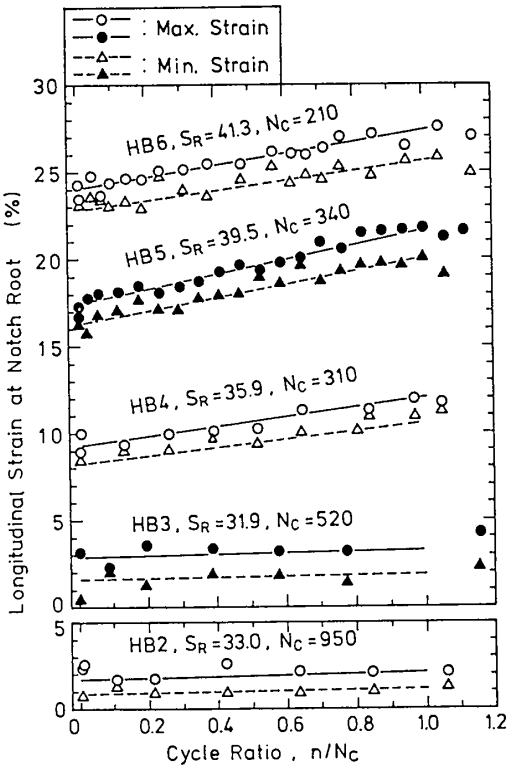

Fig. 5 Cyclic Characteristics of Longitudinal Strain at the Tip of Notch (50 kg/mm² High Strength Steel; K_t=10)

2.2.2 *Comparison of Crack Initiation Lives*

In Figs. 3, 4 and 5 it is seen that peak strains measured by Moiré method at the tip of a notch fall in a scatter band. Faired curves were drawn for each group of data as shown by solid and dotted lines, and then these curves were used as maximum and minimum limits of strain history which should be duplicated in strain cycling test of a hourglass specimen. In other words, the maximum and minimum strains in each strain cycling of a hourglass specimen were traced on these curves. Visible crack initiation life of a hourglass shaped specimen strain cycled in such a way was defined as number of cycles to formation of a surface crack 0.2 to 0.5 mm long, and symbolized as $N_c(H)$.

In Fig. 6, the relations between $N_c(H)$ and $N_c(P)$ are plotted in log-log scale. It is seen that data for mild steel specimens with K_t of 5 and 10 fall about a dotted line, that represents equal life of both specimens. While, data for mild steel specimens with K_t of 14 and those for 50 kg/mm² high strength steel specimens with K_t of 10 show the tendency that $N_c(P)$ is much shorter than $N_c(H)$. Another observation of Fig. 6 suggests that the ratio of $N_c(P)$ to $N_c(H)$ becomes smaller as the K_t of a notch in a wide plate increases.

The reason for this tendency is probably found partly in the definition of crack initi-

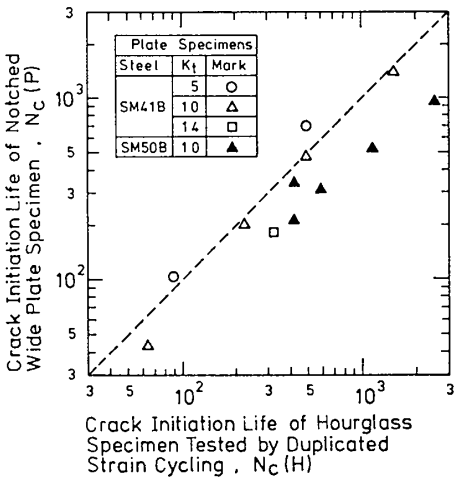

Fig. 6 Correlations between Crack Initiation Life of Notched Wide Plate and that of Hourglass Specimen Fatigued by Duplicated Strain Cycling

ation life and partly in the difference in crack initiation behaviour in notched wide plates. Crack initiation life is closely related to the size of crack. An example is given in Fig. 7, that was obtained by reversed strain cycling of hourglass specimens of a 60 kg/mm² high strength steel[13),14)]. It is clearly observed that the initiation life of a surface crack 0.01 to 0.05 mm long $N_{0.01}$ is much shorter than that of a surface crack 0.2 to 0.5 mm in length N_c.

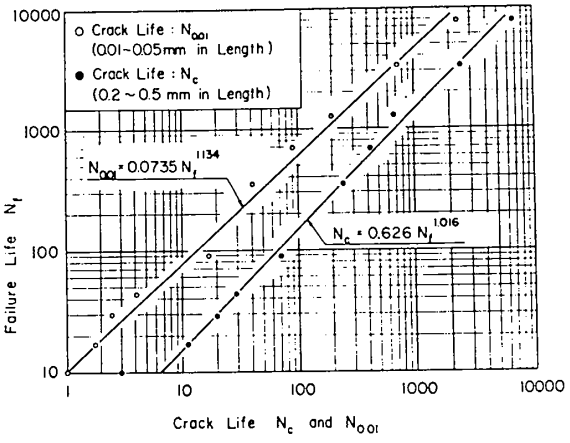

Fig. 7 Relations between Crack Initiation Life and Failure Life (60 kg/mm² High Strength Steel; Hourglass Shaped Specimen; Reversed Strain Cycling with Constant Strain Amplitude)

As described above the crack initiation behaviour in a notched plate differs widely by many factors, among which the degree of restraint in thickness direction is an impossible factor to reproduce in strain cycling test of a hourglass specimen.

If it is necessary, by all means, to get an equal life between a wide plate specimen with a sharp notch and a hourglass specimen, it may be necessary to make a sliding change of the definition of crack initiation life for the notched wide plate specimen, corresponding to the increasing K_t value.

Iida et al.[15)] carried out reversed, constant amplitude strain cycling test on the similar materials as used in the present test, and obtained the following relations;

For a mild steel, SS41E steel in JIS Code,

$$\epsilon_{ta}=0.322(N_c)^{-0.670}+0.0051(N_c)^{-0.130} \quad (1)$$

For a 50 kg/mm² high strength steel, SM50B steel in JIS Code

$$\epsilon_{ta}=0.320(N_c)^{-0.616}+0.0053(N_c)^{-0.124} \quad (2)$$

In Fig. 8, $N_c(P)$ is plotted against the crack initiation life of hourglass specimen tested by constant amplitude strain cycling, that is calculated by substituting total strain range at a half of crack initiation life of a notched wide plate into eqs. (1) and (2). Agreement between the equal life line, the

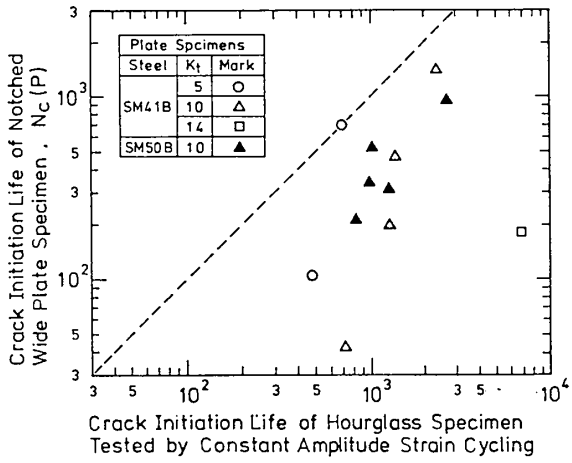

Fig. 8 Correlation between Crack Initiation Life of Notched Wide Plate and that of Hourglass Specimen Fatigued by Constant Amplitude Strain Cycling

dotted line, and data is poor, and comparison of Figs. 6 and 8 suggests that mean strain increasing at the tip of a notch is remarkably influencing factor in the prediction of crack life of a notched plate in lower cycle range.

2.2.3 *Prediction Formulas of Crack Initiation Life of Notched Wide Plate*

Some formulas have been proposed to predict the effect of mean strain in strain cycling on the low cycle fatigue life. Among these formulas the following expression given by Sachs et al.[16] is the simplest.

$$N_f=[(\epsilon_f-\epsilon_m)/\epsilon_{tR}]^m \qquad (3)$$

where m is a material constant. By replacing N_c with N_f, the damage rate per cycle will be represented by

$$[\epsilon_{tR}/(\epsilon_f-\epsilon_m)]^m \qquad (4)$$

when the sum of the value of eq. (4) becomes to unity, it means the crack initiation. Based on this concept, the crack initiation life of a notched wide plate is discussed as follows.

Letting ϵ_0 be the local strain at the notch root at the time of crack initiation in a notched plate, ϵ_{m0} be the mean strain at the first cycle, and ϵ_{tRi} and $\Delta\epsilon_{mi}$ be the total strain range and the increase rate per cycle of mean strain at i-th cycle, respectively, the following assumptions are made:

(1) The damage rate at i-th cycles is expressed by

$$[\epsilon_{tRi}/(\epsilon_0-\epsilon_{m0})]^{p_i} \qquad (5)$$

and the crack initiation life is given by N satisfying the equation

$$\sum_{i=1}^{N}[\epsilon_{tRi}/(\epsilon_0-\epsilon_{m0})]^{p_i}=1 \qquad (6)$$

(2) Effects of increasing mean strain are involved in p_i and thus p_i is a function of $\Delta\epsilon_{mi}/\epsilon_{tRi}$.

(3) Effects of the degree of restraint in thickness direction are involved in ϵ_0.

In order to define the functional expression of p_i, strain cycling test, of which procedure is shown schematically in Fig. 9, were carried out by using hourglass specimens of the same material as used for notched plate specimens. Before the cycling test the specimen was loaded by static tension up to the static tensile prestrain of 15%, and then the specimen was strain cycled with the constant total strain range of 2%, while the increasing rate of mean strain was varied for each specimen. The experimental results are shown in Fig. 10, in which results by constant mean strain are also plotted. From the results the following expressions were obtained approximately:

$$p=a[1-(\Delta\epsilon_m/\epsilon_{tR})]^4+1 \qquad (7)$$

$a=0.92$ for SM41 Steel, and
$a=0.82$ for SM50 Steel.

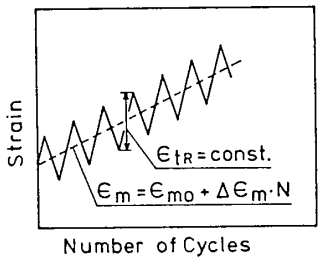

Fig. 9 Schema of Strain Cycling Test with Linear Increase of Mean Strain

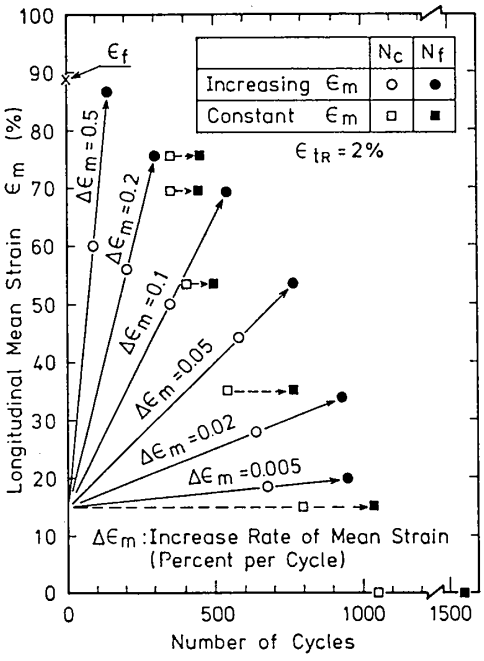

Fig. 10 Results of Strain Cycling Test with Linear Increase of Mean Strain (Hourglass Specimen; $\epsilon_{tR}=0.02$)

Thus, p_i in the formulas (5) and (6) becomes

$$p_i=a\,[1-(\Delta\epsilon_{mi}/\epsilon_{tRi})]^4+1 \qquad (8)$$

As described above, cyclic behaviour of peak strain at the notch root showed approximately linear increasing tendency for SM50 steel specimens, while the increase rate of peak strain was not constant in case of the SM41 steel specimen. However, simplification was made with the assumption that peak strains at the maximum and the minimum of each cycle behave linear increase with constant strain range from the second cycles to crack initiation life. Thus, eq. (6) is modified to

$$D=N_c\,[\epsilon_{tR}/(\epsilon_0-\epsilon_{m0})]^p$$
$$p=a\,[1-(\Delta\epsilon_m/\epsilon_{tR})]^4+1 \qquad (9)$$

$a=0.92$ for SM41 steel, and
$a=0.82$ for SM50 steel.

If eq. (9) is valid, D should become unity. But it was found that D values for all the specimen tested were ranged from 0.391 to 1.334.

Besides eq. (3) proposed by Sachs et al.[16], Ohji et al.[17], Yao-Munse[18] and Iida et al.[19] proposed prediction formulas for mean strain effects in strain cycling fatigue as follows:
By Ohji et al.,

$$N_f=[(\epsilon_f)^m-(\epsilon_m)^m]\,/4(\epsilon_{tR}/2)^m \qquad (10)$$

By Yao-Munse,

$$\sum_{i=1}^{N}[(\Delta\epsilon_t/\Delta\epsilon_{t1})^p]_i=1$$
$$p=1-0.86(\Delta\epsilon_c/\Delta\epsilon_t) \qquad (11)$$

By Iida et al.,

$$1-(N_c/N_{c0})=[W_{1/4}(\epsilon_m+\epsilon_{pa})-W_{1/4}(\epsilon_{pa})]\,/W_f \qquad (12)$$

One problem in applying these formulas to the prediction of crack initiation life of a notched plate, where the effects of notch geometry are remarkable, is the evaluation of restraint effect in thickness direction due to a notch. Thus, ϵ_f and $\Delta\epsilon_{t1}$ in the above formulas are replaced by ϵ_0, W_f by $W_{1/4}(\epsilon_0)$ that is obtained as the energy corresponding to ϵ_0, and N_f by N_c. Moreover, the mean strain was assummed to be constant value expressed by the following:

$$\epsilon_m=\epsilon_{m0}+\Delta\epsilon_m\cdot[N_c(P)/2] \qquad (13)$$

The exponent m in eqs. (3) and (10) should be equal to the value of p given by eq. (7) applied to the case of zero mean strain. Then m is decided as 1.92 for mild steel, and 1.82 for 50 kg/mm^2 steel.

In such a way expected life to crack initiation of a notched plate N_e was calculated by substituting experimental data into the equations mentioned above. Figure 11 shows the ratios of N_e to actual crack initiation life of a notched specimen $N_c(P)$. A short vertical line crossing a bold horizontal line represents a result of calculation. The results by the analysis using the author's eq. (9) show narrowest scatter band width, of which center is situated near unity. While, the results obtained by using equations after Sachs et al., Ohji et al., Yao-Munse, and Iida et al. exhibit wider scatter in the range of higher value of $N_e/N_c(P)$, which means the unsafe prediction.

The next stage is advanced in making divisions of mean strain levels as shown in Fig. 12. In this case eq. (3) by Sachs et al.

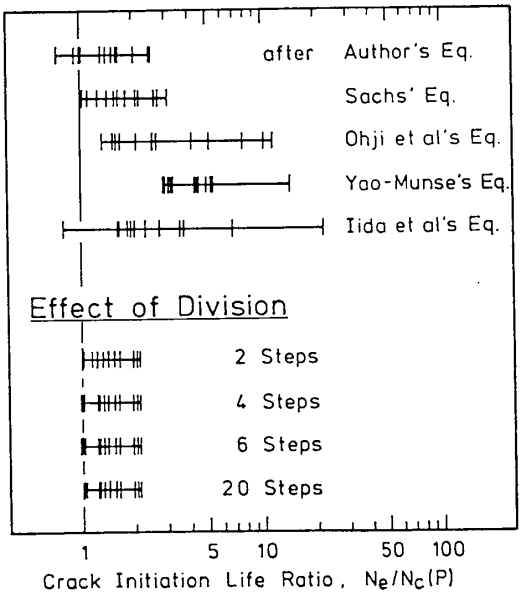

Fig. 11 Ratios of Predicted Crack Initiation Life to Actual Crack Life

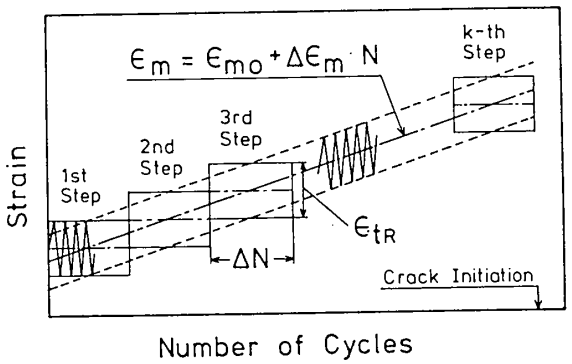

Fig. 12 Progressive Division of Increasing Mean Strain into Steps

was used by the reason of its simplest form. The results are shown in the lower part of Fig. 11. Saturating behaviour of scatter band width is observed as the number of steps becomes greater than four[20]. It, however, may be worthy of note that most of the results are distributed in unsafe side of life prediction.

3. Fatigue Strength Reduction Factor in Low Cycle Fatigue[5),8)]

3.1 *Experimental Details*

Three steels of 80 kg/mm² tensile strength and a mild steel were used in the as-received condition. Chemical compositions and tensile properties are shown in Tables 3 and 4.

Smooth and grooved solid cylinder specimens were machined out in the rolling direction of 20 and 25 mm thick 80 kg/mm² steels and of a 70 mm thick mild steel. Details of specimens used for the mild steel are shown in Fig. 13. Table 5 lists dimensions and K_t values of specimens used for 80 kg/mm² steels. Elastic stress concentration factor for a round notched specimen was calculated by the following formula[21].

$$K_\beta = 1 + (K_0 + 1)\left\{1 - \left(\frac{\beta}{180}\right)^{1+2.4\sqrt{R/h}}\right\} \quad (14)$$

where K_0=theoretical stress concentration factor in case of notch angle of 0°

K_β=theoretical stress concentration factor in case of notch angle of β°

h=remainder subtracted radius of minimum section from radius of parallel part

R=notch radius.

Peterson's charts[12)] were used for hourglass shaped specimens and for K_0 values. The specimen surface was polished with emery paper of very fine grain and finished with buffing cloth.

Diametral natural strain amplitude was controlled for the fatigue tests of high tensile steel specimens under the reversed cycling condition. The change of diameter at the minimum cross section of a specimen was detected by an unbonded type wire strain gauge or by a linear differential transformer.

In the fatigue tests of mild steel specimens both diametral natural strain amplitude at the test section of a specimen and axial load applied were controlled under the reversed cycling condition.

All specimens were tested at ambient temperature by triangular shaped cycling. The cycling rate was kept about 2 to 5 cpm when the number of cycles to failure was expected to be less than 100 cycles, while 5 to 10 cpm in other cases. In general, loading was started with tension phase.

In order to make continuous record of cyclic behaviour of longitudinal strain on the surface of the test section, strain gauges of 0.2 mm in gauge length were bonded longitudinally with the transverse centerline of the gauge located at the minimum cross section, that is notch root of grooved cylinder specimen of mild steel, while strain gauges of 3 mm in gauge length were applied on the center of hourglass shaped, mild steel specimen.

3.2 *Results and Discussion*

3.2.1 *Static Tensile Properties*

Two to five specimens in each test series were tested in static tension. An example of the results is shown in Fig. 14, in which tensile properties are plotted against elastic stress concentration factor. It is found that true fracture stress increases gradually and reaches to the saturated value at the K_t value of nearly 2.5 with the increase of K_t

Table 3 Chemical Compositions of Steels (Ladle and Check Analyses; Percent by Weight)

Steel	Steel Code	C	Si	Mn	P	S	Ni	Cr	Mo	Cu	Analysis
80 kg/mm² High Ten. Steel	8M	0.15	0.20	0.85	0.019	0.008	—	1.05	0.48	0.30	Ladle
	8NA	0.16	0.28	0.36	0.015	0.007	2.25	1.20	0.42	—	Check
	8NB	0.10	0.23	0.60	0.019	0.009	2.65	0.47	0.45	—	Check
SM41A	4M	0.17	0.24	0.60	0.015	0.015	—	—	—	—	Ladle

Table 4 Tensile Properties of Steels (Mean Value; Cylindrical Specimen)

Steel Code	K_t[1]	σ_y (kg/mm²)	σ_u (kg/mm²)	σ_f (kg/mm²)	ϵ_f
8M	1.01	76.2	88.2	167.8	1.034
8M	1.11	83.7	96.7	169.2	0.807
8NA	1.11	85.2	96.3	169.2	0.998
8NB	1.11	79.3	86.6	163.7	1.071
4M	1.06	28.2	58.3	111.3	0.794

1) Shape Factor (Theoretical Elastic Stress Concentration Factor) of Specimen

Table 5 Dimensions and Shape Factors of Specimens Used for 80 kg/mm² Steels

Code	K_t[1]	d[2] (mm)	R[3] (mm)	Remarks[4]
8MA	1.01	8	80	HG
8MU	1.11	7	14	HG
8MB	1.57	8	2.4	RN
8MC	2.48	8	0.6	RN
8MD	3.48	8	0.25	RN
8NA	1.11	7	14	HG
8NAN	2.35	7	0.6	RN
8NB	1.11	7	14	HG
8NBN	2.35	7	0.6	RN

1) Elastic Stress Concentration Factor
2) Diameter of Test Section
3) Notch Radius
4) HG=Hourglass Type Specimen (Solid)
RN=Round Notch Specimen (Grooved, Solid)

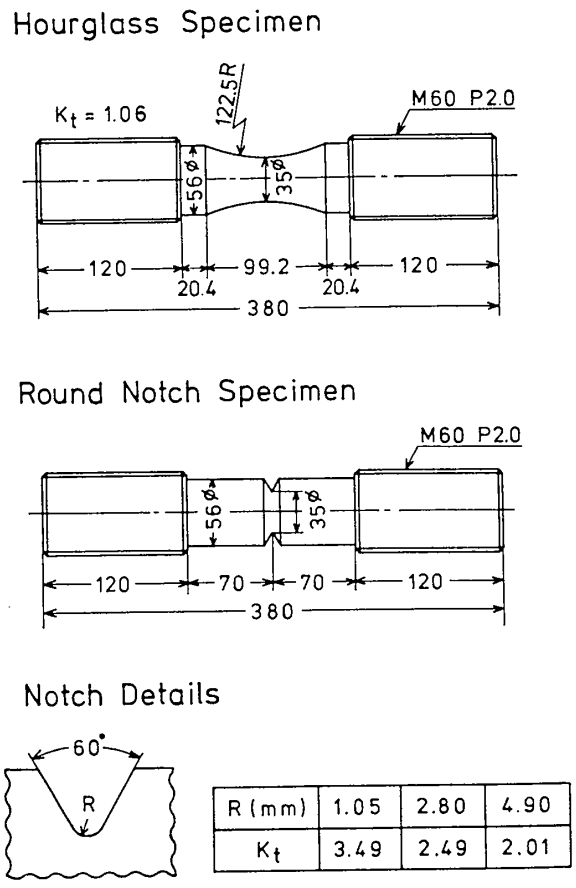

R (mm)	1.05	2.80	4.90
K_t	3.49	2.49	2.01

Fig. 13 Details of Specimens

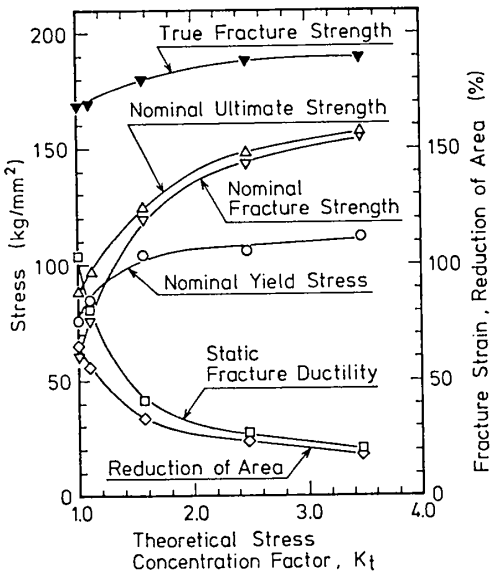

Fig. 14 Relations between Tensile Properties and Shape Factor of Specimen (80 kg/mm² Steel)

value. On the other hand, curves of static fracture ductility and nominal ultimate tensile strength show steep change up to the K_t value of approximately 1.6, and thereafter gradual change with the increasing K_t.

3.2.2 *Crack Initiation Life as a Function of Equivalent Strain Amplitude*

Letting d_t and d_c be diameters of the test section at the maximum tensile and compressive axial deformations, respectively, diametral natural total strain amplitude, ϵ_{ta}^d, that is the controlling value in diametral strain controlled, reversed fatigue test, is given as follows:

$$\epsilon_{ta}^d=(1/2)\,ln\,(d_c/d_t) \tag{15}$$

Then, longitudinal natural plastic, elastic and total strains, ϵ_{pa}, ϵ_{ea} and ϵ_{ta}, are obtained with the assumption of constant volume in plastic deformation, for an hourglass shaped specimen:

$$\epsilon_{ta}=\epsilon_{pa}+\epsilon_{ea}=2\epsilon_{ta}^d+\left(\frac{1}{2}-\nu\right)\frac{\sigma_R}{E} \tag{16}$$

where ν=Poisson's ratio (=0.3)

E=Young's modulus (=21000 kg/mm²)

σ_R=longitudinal true stress range in the stable condition, where cyclic hardening and softening behaviours have disappeared.

As described above strain gauges were bonded, before the fatigue test, at the test section of mild steel specimens. Results of strain measurement on hourglass shaped specimens showed fair agreement with the calculated value by eq. (16) within the error range of ±10%.

Results of diametral strain controlled fatigue test on hourglass shaped specimens of mild steel are shown in Fig. 15, in which longitudinal natural strain amplitude is plotted against number of cycles to initiate a surface crack 0.2 to 0.5 mm long, N_c, and failure life, N_f. Linear relations are easily observed for ϵ_{ea} versus N_c and ϵ_{ta} versus N_c curves, while plastic strain amplitude does not exhibit linear decrease, in log-log plot, against increasing N_c. Such phenomenon was previously pointed out by Hotta et al.[22], who concluded: (1) Steels with banite and tempered martensite structures show a convex curve of ϵ_{pa} versus N_c, and (2) Steel, of which tensile strength is lower than 60 kg/mm², with ferrite and ferrite-perlite structures shows a straight line relation between ϵ_{pa} and N_c. According to the conclusion by Hotta et al., ϵ_{pa} versus N_c curve in Fig. 15 should be a straight line, because steel tested is a mild steel. Curved relation, however, is shown for no reason that could be discovered.

As for a round notched specimen, by introducing radial strain amplitude, ϵ_{ta}^r, the following formula is found with the assumption of constant volume.

$$\epsilon_{ta}+\epsilon_{ta}^d+\epsilon_{ta}^r=0 \tag{17}$$

The ϵ_{ta} can be measured by strain gauge of short gauge length, and ϵ_{ta}^d is the control value, then ϵ_{ta}^r is given by eq. (17). Thus, equivalent strain amplitude, $\epsilon_{eq,a}$ is calculated by

$$\epsilon_{eq,a}=\frac{\sqrt{2}}{3}\{(\epsilon_{ta}-\epsilon_{ta}^d)^2+(\epsilon_{ta}^d-\epsilon_{ta}^r)^2+(\epsilon_{ta}^r-\epsilon_{ta})^2\}^{1/2} \tag{18}$$

In Fig. 16, the results of diametral strain

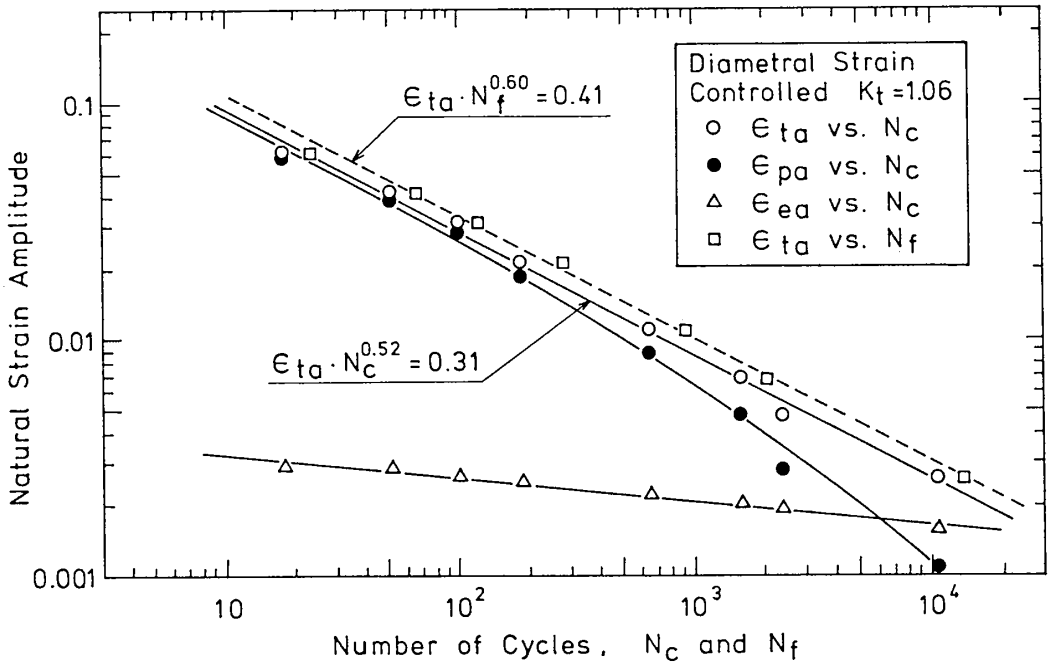

Fig. 15 Relations between Longitudinal Strain Amplitude and Fatigue Life (Mild Steel; Hourglass Specimen)

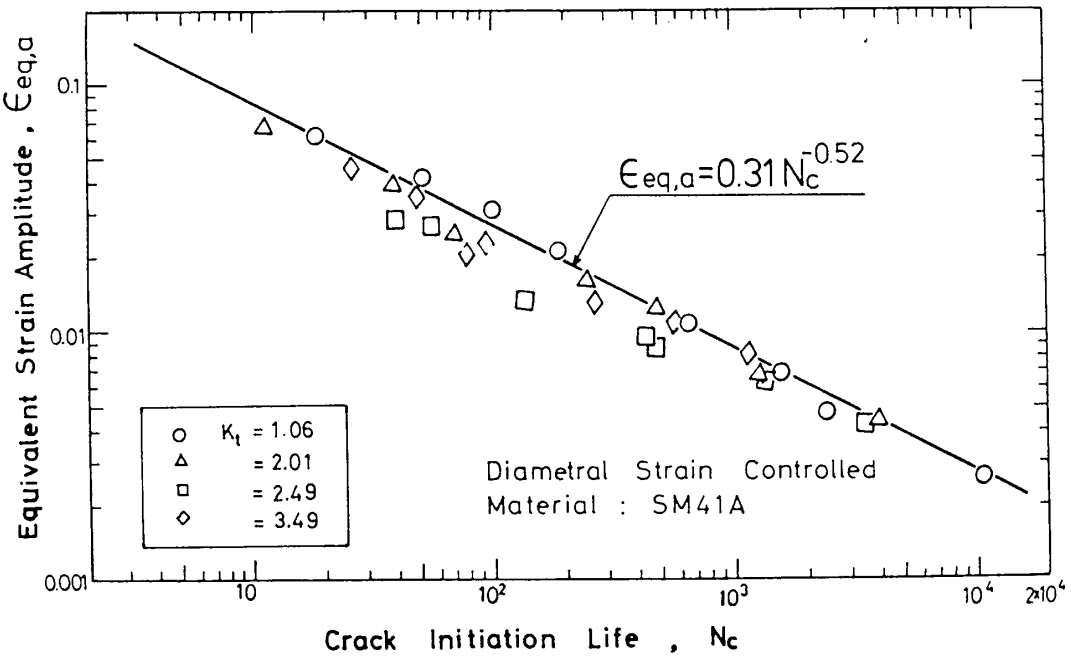

Fig. 16 Equivalent Strain Amplitude versus Crack Initiation Life for Notched Mild Steel Specimens

controlled fatigue tests of grooved cylinder specimens are plotted in the form of $\epsilon_{eq,a}$ against N_c. The solid line represents the ϵ_{ta} versus N_c curve for hourglass specimen. Fair agreement can be seen between the solid line and results of notched specimens, excepting data for K_t=2.49 in the N_c range less than 400 cycles. This observation may lead, as the first approximation, to a conclusive remark that, regardless of specimen

geometry, a fatigue crack will initiate at an approximately same life, if the equivalent strain amplitude at a notch root is equal. Moreover, it may be concluded that the fatigue strength reduction factor is approximately equal to dynamic, plastic strain concentration factor. The comparison of the former with the latter showed fair agreement all over the range of nominal stress amplitude in the test. Incidentally, the dynamic, plastic strain concentration factor can be obtained by a comparatively easy method, of which principle was previously proposed by Manson and Hirschberg[4]. The method needs one of the following formulas[23-25] and dynamic true stress-natural strain diagram, that is obtained from data on the relation between strain range and stress range in the stable condition during the strain cycling test of the hourglass specimen.

$$K_\sigma = K_\epsilon/(K_\epsilon - K_t + 1) \tag{19}$$

$$K_\sigma \cdot K_\epsilon = (K_t)^2 \tag{20}$$

3.2.3 *Fatigue Strength Reduction Factor in Low Cycle Fatigue*

In low cycle fatigue a specimen is loaded beyond the yield stress. Thus, even if the specimen has no or little stress concentration, the controlling value, strain amplitude or stress amplitude, should be carefully selected from the viewpoint of design use. In case of the notched specimen, the problem will be more complex, because strain distribution along the notched section is not simple as the case of the smooth specimen.

Different opinions[2-5,8,26-28] on the appropriate way of low cycle fatigue test of grooved cylinder specimen have been reported to obtain reliable information about the application of laboratory test results to fatigue design. Table 6 summarizes various methods proposed previously.

The method after Manson and Hirschberg[4] needs a series of reversed, diametral strain-controlled tests of smooth specimens and then a series of load-controlled test of notched

Table 6 Definitions of Fatigue Strength Reduction Factor

Method by	Control Value[1]	Test Procedure[2]	Use of Dynamic Stress vs. Strain Curve for Smooth Specimen[3]	Definition[4]	Result[5]
Manson et al.	ϵ(S) L(N)	(1) SCT of SS (2) LCT of NS	—	—	$(K_f \fallingdotseq K_\epsilon)$
Iida	ϵ(S) ϵ(N)	(1) SCT of SS (2) SCT of NS	—	ϵ(S)/ϵ(N)	$K_f > K_t$
Krempl Ia	ϵ(S) L(N)	(1) SCT of SS (2) LCT of NS	S(N)→ϵ*(N)	ϵ(S)/ϵ*(N)	$K_f > K_t$
Krempl Ib	ϵ(S) L(N)	(1) SCT of SS (2) LCT of NS	ϵ(S)→S*(S)	S*(S)/S(N)	$K_f < K_t$
Krempl II	ϵ(S) L(N)	(1) SCT of SS (2) LCT of NS	—	E×ϵ(S)/S(N)	$K_f > K_t$
Stress Amp.	L(S) L(N)	(1) LCT of SS (2) LCT of NS	—	S(S)/S(N)	$K_f < K_t$
Present Paper	ϵ(S) ϵ(N)	(1) SCT of SS (2) SCT of NS	—	ϵ_{eq}(N)/ϵ(S)	$K_f > K_t$ $K_f \fallingdotseq K_\epsilon$

1) ϵ( ): strain amplitude, L( ): load (=nominal stress) amplitude, (S): smooth specimen, (N): notched specimen. For example, ϵ(S) means strain amplitude for smooth specimen.
2) SCT: (diametral) strain controlled test, LCT: load controlled test, SS: smooth specimen, NS: notched specimen.
3) ϵ*(N) and S*(S) are obtained by a stress-strain diagram as a corresponding value to S(N) and ϵ(S), respectively.
4) ϵ_{eq}: equivalent strain amplitude
5) K_f: fatigue strength reduction factor, K_t: theoretical elastic stress concentration factor, K_ϵ: plastic strain concentration factor

specimens. In the latter test series, a notched specimen is loaded by duplicating a stress range against cycle history that has been obtained by strain cycling a smooth specimen. Manson and Hirschberg tested a 7075-T6 aluminum alloy and a 4340 steel by this method, and discussed the agreement of predicted crack initiation life of notched specimen with experimental results. Fatigue strength reduction factor in low cycle range K_f is not defined in their paper, but experimental results seem to suggest that K_f is nearly equal to plastic strain concentration factor K_ϵ.

In the method after Iida[5] reversed, diametral strain controlled tests are carried out for both smooth and notched specimens. By applying eqs. (15) and (16), longitudinal strain amplitude against crack initiation life curves are constructed for both specimen series, and K_f is defined, as shown in the upper schema in Fig. 17, as the ratio of longitudinal strain amplitude for smooth specimen at a certain N_c to that for notched specimen at the same N_c. One problem in this method is found, as pointed out by Krempl[29], in the method of conversion of longitudinal strain amplitude from the controlled value of diametral strain amplitude. The fact of a complex state of strain distribution along the notched section suggests that experimental results by this type of testing may limit its application for specific cases.

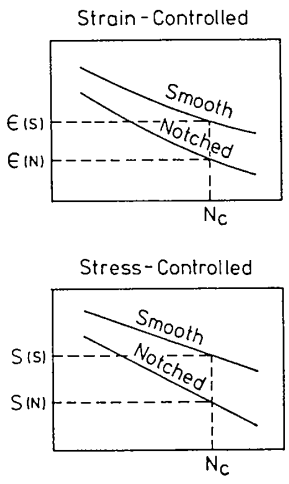

Fig. 17 Schemata for Definition of Fatigue Strength Reduction Factor

Krempl[3),26),27)] studied the influence of the definition of the fatigue strength reduction factor on its magnitude, after discussing the various probabilities of defining this factor. The method adopted by Udoguchi and Wada[28], who derived the conclusion that K_f is nearly equal to K_t, is very similar to Krempl's method *Ia*. Krempl's methods are based on results by reversed, true strain-controlled fatigue test of smooth or hourglass shaped specimens and results by reversed, load-controlled tests of grooved cylinder specimens.

In the Krempl's method *Ia*, the nominal strain range of the notched specimen is obtained from the nominal stress range by using a cyclic true stress-natural strain diagram for the smooth specimen, or monotonic diagram in case of lack of data. The K_f is defined as the ratio of the strain range such defined to the strain range of smooth specimen.

In the method *Ib* by Krempl, the stress range of the smooth specimen is figured from the strain range via a suitable stress-strain diagram. The ratio of the stress range such obtained to the stress range of the notched specimen, that is the control value in the test, is defined as the K_f.

The K_f by Krempl's method *II* is defined as the ratio of fictitious stress range of the smooth specimen, that is obtained by multipling Young's modulus by the strain range in the test of smooth specimen, to the nominal stress range in the test of the notched specimen.

Three problems related to Krempl's methods may be posed here: (1) Essential difference of cyclic characteristics of stress and strain diagrams in load- and strain-controlled fatigue. In the strain-controlled fatigue, the maximum and the minimum stresses vary with cycles due to cyclic hardening and softening, and in the case of load-controlled test the behaviour is the reverse, (2) True stress versus natural strain

diagram for a notched specimen differs much from that for smooth specimen, and (3) The converted strain used in the *Ia* is a kind of nominal and averaged strain, that does not correspond to the realistic surface strain at the notch root.

Methods proposed by Manson et al., Iida and Krempl and others are based on a few assumptions respectively, and have points of discussion. It may be worthy to cite here Krempl's opinion[29] that there is, at present, no best way to obtain low cycle fatigue design information which would satisfy all the requirements.

The simplest difinition of K_f is shown in the second frame from the bottom of Table 6 and in the lower schema in Fig. 17. In this case both smooth and notched specimens are load-controlled and K_f is defined as the ratio of nominal net section stress amplitudes. Physical meanings of this method is clear in the case where a structural component with discontinuity is subjected to load-controlled condition.

Setting aside the discussion, fatigue strength reduction factors for the mild steel tested were calculated as a function of the nominal stress amplitude. Results by Iida's method are shown in Fig. 18, in which the tendency of larger K_f is observed in the whole range of the abscissa. Figures 19 to 21 are results by Krempl's methods. The K_f values by Krempl's methods of *Ia* and *II* are always larger than K_t, while K_f by the method *Ib* gives smaller value than K_t. Direct method comparing stress amplitudes in load-controlled fatigue tests of smooth and notched

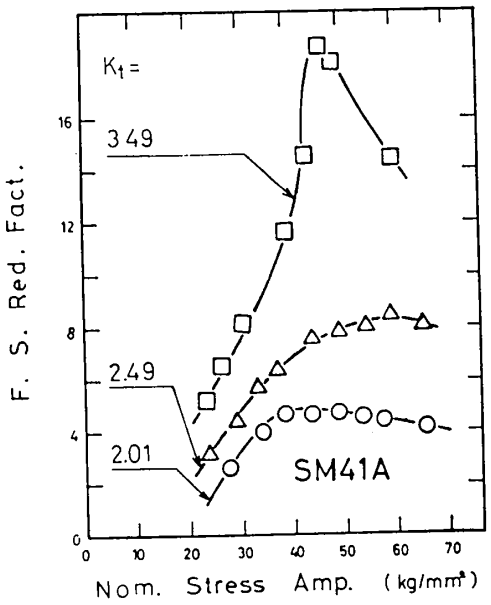

Fig. 18 Fatigue Strength Reduction Factor by Iida's Method as a Function of Nominal Stress Amplitude (Mild Steel)

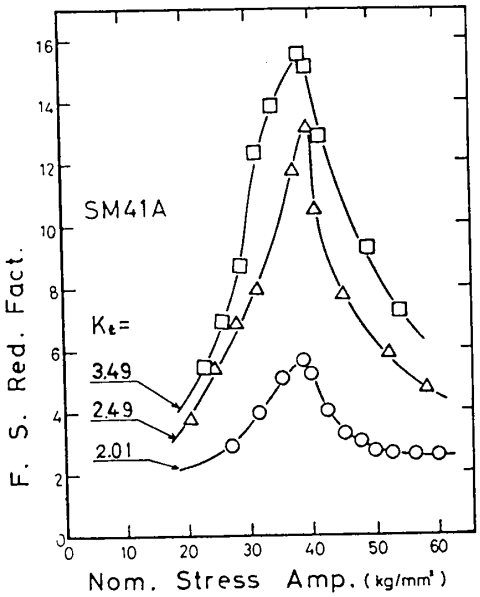

Fig. 19 Fatigue Strength Reduction Factor by Krempl's *Ia* Method as a Function of Nominal Stress Amplitude (Mild Steel)

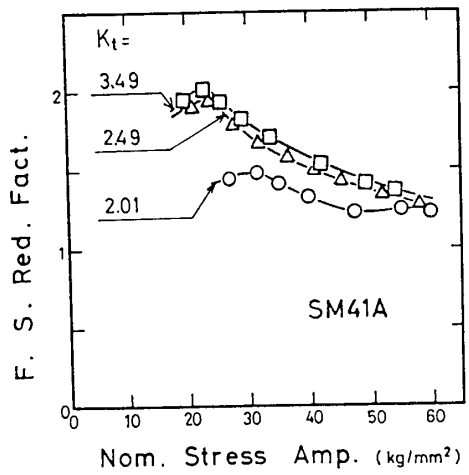

Fig. 20 Fatigue Strength Reduction Factor by Krempl's *Ib* Method as a Function of Nominal Stress Amplitude (Mild Steel)

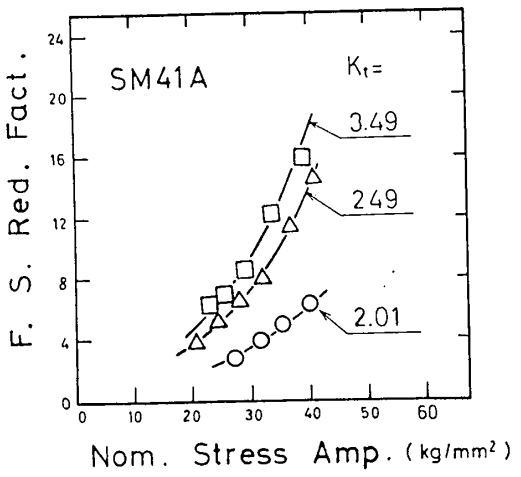

Fig. 21 Fatigue Strength Reduction Factor by Krempl's *II* Method as a Function of Nominal Stress Amplitude (Mild Steel)

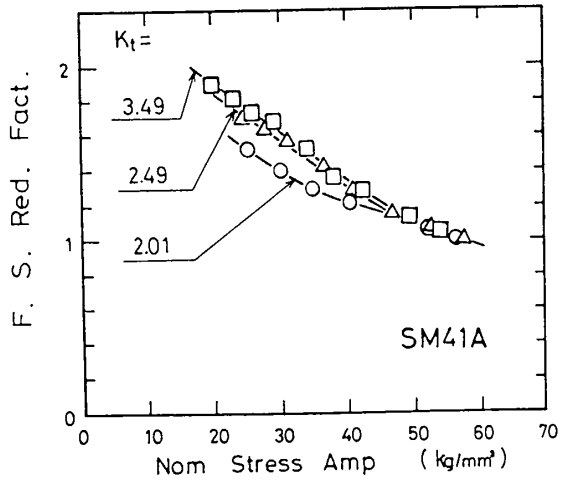

Fig. 22 Fatigue Strength Reduction Factor by Comparing Method of Nominal Stress Amplitudes in Load-Controlled Tests (Mild Steel)

specimens shows smaller K_f than K_t.

3.2.4 *The A-Factor*

The A-factor defined in USA Standard, USAS-B31.7 (1969), is expressed as follows:

$$A=(K_f-K_t)/(K_t-1) \qquad (21)$$

This factor is calculated from the test results for the mild steel and plotted in Fig. 23, in which A-factor curve described in the USAS B31.7 for cabon steel (p-Number 1, ASME IX) is also shown by a dot-dash line. In this case solid curves were calculated by

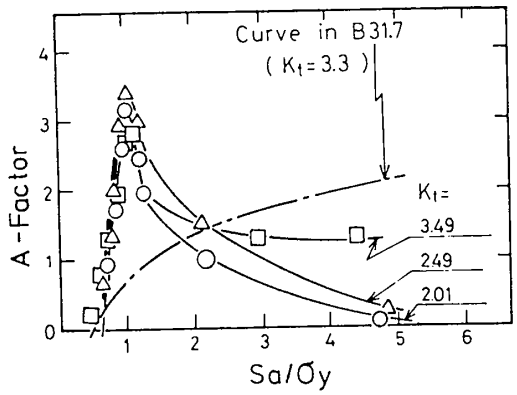

Fig. 23 A-Factors versus Modified Stress Amplitude (Mild Steel)

substituting K_f values calculated by the method described in the last part of section 3.2.2. Large discrepancy is observed excepting the point of 2.2 of the ratio of stress amplitude to yield stress. This observation may suggest necessity of further studies on the definition of low cycle fatigue strength reduction factor for design use.

4. Conclusions

Repeated (zero-to-tension) load-controlled fatigue tests were carried out in low cycle fatigue range on center notched wide plate specimens of mild and 50 kg/mm² strength steels. Maximum and minimum strain histories against cycles were measured by Moiré method at the tip of a notch, and these histories were duplicated in strain cycling of hourglass specimens of the same material. The following conclusions can be drawn from the results of the tests:

(1) Crack initiation behaviour of a notched wide plate is influenced by the four factors: the maximum peak strain at the first half cycle, amplitude of peak strain, increasing mean strain at the tip of a notch and the degree of restraint in thickness direction.

(2) In cases of mild steel specimens with a notch of 5 and 10 in elastic stress concentration factor, good correlations are found between the crack initiation life of the notched plate and that of hourglass shaped specimen, which was strain cycled by duplicating strain histories at the tip of notch in

the wide plate. While correlation is not so good for the cases of mild steel specimens with a notch of 14 in elastic stress concentration factor and for 50 kg/mm^2 strength steel specimens.

(3) Poor correlation is found between the crack initiation life of the notched wide plate and that of the hourglass shaped specimen fatigued by strain cycling with constant mean strain.

(4) An expression predicting cumulative damage in a notched wide plate was derived on the basis of results of strain cycling tests on hourglass specimens with linear increase of mean strain. The ratio of the predicted crack initiation life, that is calculated by the derived expression, to that of the actual crack life of a notched wide plate ranges from approximately 0.75 to 2.5. Nevertheless the scatter width of the predicted-to-actual crack life ratio is narrowest for the present method, as compared with the results obtained by using previously proposed formulas expressing the effect of mean strain.

(5) In case where a previously proposed formula predicting effects of mean strain is used for prediction of the crack initiation life of the notched wide plate, the scatter band width of predicted-to-actual crack life ratios saturates with the increasing number of divisions in the method of replacing linear increase of mean strain by arbitrary number of steps with progressively increased mean strain. In the present paper four steps were enough to minimize the scatter band width. However, the predicted-to-actual crack life ratio derived by this method gives in general the prediction of unsafe side.

Completely reversed strain cycling tests on a mild and 80 kg/mm^2 steels and completely reversed load cycling tests on a mild steel were carried out, in low cycle fatigue range, by using hourglass shaped and grooved cylinder specimens. From the tests results conclusions can be drawn as follows:

(1) A visible surface crack 0.2 to 0.5 mm long initiates at an approximately same number of cycles at the notch root of a grooved cylinder specimen with any shape factor, if the equivalent strain amplitude at the notch root is equal. And the crack initiation life of a grooved cylinder specimen is nearly equal to that of an hourglass specimen, if the equivalent strain amplitude for the former is equal to the longitudinal total natural strain amplitude for the latter.

(2) Fatigue strength reduction factor defined by strain cycling tests of smooth and grooved specimens is equal, in principle, to the plastic strain concentration factor at the notch.

(3) The fatigue strength reduction factor K_f derived by Krempl's method *Ib* shows smaller value than the elastic stress concentration factor of a notch K_t. While, K_f values by Krempl's methods *Ia* and *II* and by Iida's method are larger than K_t value.

(4) Fatigue strength reduction factor defined by load cycling tests of smooth and grooved cylinder specimens is always lower than the K_t value.

Acknowledgement

The kind cooperation by Prof. Y. Ando, Dr. I. Soya and Dr. Y. Urabe is greatefully acknowledged. The author is indebted to Prof. K. Nagai, Prof. M. Iwata and Dr. S. Nishimura for their proper guidance for application of the Moiré method. Assistance extended from Prof. K. Miya, Dr. Y. Fukuda and expert help of Mr. M. Kurosawa and others are highly appreciated. Also thanks are due to Mr. Y. Kho for his excellent help in preparation of the present manuscript.

References

1) CREWS, Jr., J. H. and HARDRATH, H. F.: "A Study of Cyclic Plastic Stresses at a Notch Root," Exp. Mech., June, 1966
2) TAGART, Jr., S. W.: "Plastic Fatigue Analysis of Pressure Components," ASME Paper 68-PVP-3 (1968)
3) KREMPL, E.: "Reactor Primary Coolant Rupture Study," Quart. Prog. Rep. Nos. 3 and 10, AEC Res. Devel. Rep. GEAP-5082 (1966) and GEAP-5554 (1967)
4) MANSON, S. S. and HIRSCHBERG, M. H.: "Crack Initiation and Propagation in Notched

Fatigue Specimens," NASA TMX-52126 (1965)
5) IIDA, K.: "Notch Effect on Strain-Controlled Low Cycle Fatigue Strength of 80 kg/mm² High Tensile Steel," J. Soc. of Naval Architects of Japan, Vol. 119 (1966) (In Japanese)
6) ANDO, Y., IIDA, K. and SOYA, I.: "Initiation and Propagation of a Crack and Cyclic Behavior of Strain in Low-Cycle Fatigue—Correlation between a plate specimen with a notch and a bar specimen—," J. Soc. of Naval Architects of Japan, Vol. 128 (1970) (In Japanese)
7) ANDO, Y., IIDA, K. and SOYA, I.: "An Investigation of Low Cycle Fatigue Life of Wide Plate with a Notch," J. Soc. of Naval Architects of Japan, Vol. 129 (1971) (In Japanese)
8) IIDA, K., URABE, Y. and ANDO, Y.: "Low Cycle Fatigue Strength Reduction Factor for a Mild Steel," J. Soc. of Naval Architects of Japan, Vol. 130 (1971) (In Japanese)
9) NISHIDA, M.: "Stress Concentration," Morikita-Shuppan (1967) (In Japanese)
10) NAGAI, K., OHTSUKA, A. and OGAWA, K.: "Behaviors of Plastic Strain of Steels Subjected to Low-Cycle Pulsating Tension," J. Soc. of Naval Architects of Japan, Vol. 124 (1968) (In Japanese)
11) BOSSAERT, W., DECHAENE, D. and VINCKIER, A.: "Computation of Finite Strains From Moiré Displacement Patterns," J. of Strain Analysis, Vol. 3, No. 1 (1968)
12) PETERSON, R. E.: "Stress Concentration Design Factors," John Wiley & Sons, Inc. (1962)
13) IIDA, K.: "Crack Initiation Life and Microfractographic Analysis in Strain Cycling Fatigue," Trans. Japan Welding Society, Vol. 2, No. 1 (1971)
14) IIDA, K.: "Crack Initiation Life in Low Cycle Fatigue," First International Symposium of the Japan Welding Society, Paper No. IIIA7 (1971)
15) IIDA, K., FUKUDA, Y. and ANDO, Y.: "Strain Cycling Fatigue of Welds of Ship Structure Steels," International Institute of Welding, Doc. No. XIII-534-69 (1969)
16) SACHS, G., GERBERICH, W. W., WEISS, V. and LATORRE, J.V.: "Low-Cycle Fatigue of Pressure Vessel Materials," Proc. ASTM, Vol. 60 (1961)
17) OHJI, K., MILLER, W. R. and MARIN, J.: "Cumulative Damage and Effect of Mean Strain in Low-Cycle Fatigue of 2024-T351 Aluminum Alloy," J. of Basic Engineering, Dec., 1966
18) YAO, J. T. P. and MUNSE, W. H.: "Low-Cycle Axial Fatigue Behavior of Mild Steel," ASTM STP 338 (1968)
19) IIDA, K., INOUE, H., KOBAYASHI, Y. and MIYAMOTO, T.: "Effect of Mean Strain in the Diametral Strain Controlled Low Cycle Fatigue," J. Soc. of Naval Architects of Japan, Vol. 127 (1970) (In Japanese)
20) IIDA, K. and SOYA, I.: "Supplementary Analysis of Prediction Formulas of Fatigue Life," to be published
21) HEYWOOD, R. B.: "Designing by Photoelasticity," Chapman & Hall, 167/187 (1952)
22) HOTTA, T., ISHIGURO, T., ISHII, N. and SEKIGUCHI, S.: "Further Investigation on Estimation of Low Cycle Fatigue Strength of Steels (2nd Report)—On kink point in a relation of plastic strain range against failure life—," J. Soc. of Naval Architects of Japan, Vol. 126 (1969)
23) GRIFFITH, G. E.: "Experimental Investigation of the Effects of Plastic Flow in a Tension Panel with a Circular Hole," NACA TN 1705 (1948)
24) HARDRATH, H. F. and OHMAN, L.: "A Study of Elastic and Plastic Stress Concentration Factors due to Notches and Fillets in Flat Plates," NACA Report 1117 (1951)
25) NEUBER, H.: "Theory of Stress Concentration for Shear-Strained Prismatical Bodies with Arbitrary Nonlinear Stress-Strain Law," Trans. ASME, Ser. E, Dec., 1961
26) KREMPL, E.: "Notched High-Strain Fatigue Behavior of Three Low-Strength Structural Steels," Proceedings of the First Int. Conf. on Pressure Vessel Technology, Part II, ASME, 1969, 1319/1328
27) KREMPL, E.: "Low-Cycle Fatigue Strength Reduction in Notched Flat Plates," ASME paper 67-MET-13 (1967)
28) UDOGUCHI, T. and WADA, T.: "Notch Effect on Low-Cycle Fatigue Strength of Metals," Proceedings of the First Int. Conf. on Pressure Vessel Technology, Part II, ASME, 1969, 1191/1202
29) Discussions by T. UDOGUCHI and K. IIDA, and Author's Closure by E. KREMPL on the Paper Entitled: "Notched High-Strain Fatigue Behavior of Three Low-Strength Structural Steels," Proceedings of the First Int. Conf. on Pressure Vessel Technology, Part III, ASME 1969, 236/238